Original Article

A standardized protocol for clear aligner thickness measurement using a 3D-printed auxiliary device

Peiqi Wang[a]; Qingying Liu[b]; Junyan Leng[c]; Xiaoqin Zhou[d]; Peilin Li[e]; Xianglong Han[f]; Ding Bai[f]; Chaoran Xue[e]

ABSTRACT

Objectives: To develop and validate a standardized protocol for clear aligner (CA) thickness measurement using a three-dimensional (3D)-printed auxiliary device to improve measurement reliability.

Materials and Methods: 24 pairs of digital dental models (D0s) were included and 3D-printed into physical models (P0s), from which CAs were thermoformed using 0.75-mm polymer sheets. Measurement auxiliary devices (MADs) were designed on D0s through measurement point selection, direction determination, electronic gauge mapping, and base shaping, and then 3D-printed. Two operators measured CA thickness (40 points per CA, 48 CAs) using an electronic gauge both directly (direct measurement, D-M) and with MADs (auxiliary measurement, A-M) across three sessions. Measurement precision (repeatability and reproducibility) of D-M and A-M were analyzed using intraclass correlation coefficients (ICCs) and repeated-measures analysis of variance (ANOVA) or Friedman tests. Bland-Altman plots were used to evaluate intersession agreement.

Results: A-M demonstrated superior intersession repeatability with ICC $>$ 0.90 at all points and high intersession agreement with a narrow 95% limit of agreement (LoA) and minimal outliers. Interoperator reproducibility for A-M was also higher, with ICCs above 0.75 at all points, compared to D-M, which showed ICCs below 0.75 at almost all points.

Conclusions: The 3D-printed auxiliary device-based protocol provides a precise and operator-independent method for CA thickness measurement, offering a tool for quality control and providing a foundation for future research on material advancement and design optimization to improve aligner functionality. (*Angle Orthod*. 2026;00:000–000.)

KEY WORDS: Clear aligner; CAD/CAM; Measurement protocol

The first two authors contributed equally to this work.

[a] Research Associate, State Key Laboratory of Oral Diseases & National Center for Stomatology & National Clinical Research Center for Oral Diseases & Department of Orthodontics, West China Hospital of Stomatology, Sichuan University, Chengdu, China.

[b] M.D.S. Candidate, State Key Laboratory of Oral Diseases & National Center for Stomatology & National Clinical Research Center for Oral Diseases & Department of Orthodontics, West China Hospital of Stomatology, Sichuan University, Chengdu, China.

[c] B.D.S. Candidate, State Key Laboratory of Oral Diseases & National Center for Stomatology & National Clinical Research Center for Oral Diseases & Department of Orthodontics, West China Hospital of Stomatology, Sichuan University, Chengdu, China.

[d] Dentist-in-Charge, Department of Stomatology, People's Hospital of Pengshui Miao& Tujia Autonomous Country, Chongqing, China.

[e] Associate Professor, State Key Laboratory of Oral Diseases & National Center for Stomatology & National Clinical Research Center for Oral Diseases & Department of Orthodontics, West China Hospital of Stomatology, Sichuan University, Chengdu, China.

[f] Professor, State Key Laboratory of Oral Diseases & National Center for Stomatology & National Clinical Research Center for Oral Diseases & Department of Orthodontics, West China Hospital of Stomatology, Sichuan University, Chengdu, China.

Corresponding author: Dr Chaoran Xue, State Key Laboratory of Oral Diseases & National Clinical Research Center for Oral Diseases, Department of Orthodontics, West China Hospital of Stomatology, Sichuan University, 14#, 3rd, Section of Renmin South Road, Chengdu 610041, China
(e-mail: xuechaoran@scu.edu.cn)

Accepted: September 12, 2025. Submitted: November 27, 2024.
Published Online: October 15, 2025

INTRODUCTION

Clear aligners (CAs) have gained wide popularity in orthodontics by providing an esthetic, comfortable, oral hygiene-friendly alternative to traditional metal brackets.[1,2] The efficacy of CAs depends on precise engineering, particularly regarding thickness. Excessive thickness can increase force delivery on teeth, cause patient discomfort and, thus, potentially hinder desired tooth movement. Conversely, insufficient thickness may compromise the aligner's structural integrity and force application, leading to inadequate effectiveness and prolonged treatment durations.[3]

CAs are typically fabricated by vacuum thermoforming, which induces nonuniform location-dependent thickness reduction across the aligner,[4,5] significantly affecting force delivery in different regions.[6,7] Therefore, accurate thickness measurements at specific locations are fundamental to ensure that the aligners meet the required specifications for orthodontic treatment, which is crucial for quality control and clinical outcome prediction. Current measurement methods include manual measurement using electronic thickness gauges, and digital assessments on micro-computed tomography (μCT), scanning electron microscopy (SEM), or three-dimensionally (3D) scanned aligners. However, each method presents certain challenges. Specifically, 3D scanning's reliance on antireflective spray on transparent aligners can introduce measurement errors due to an uneven spray layer.[8–10] SEM requires sectioning of the aligners, potentially causing deformation and compromising material integrity.[11] μCT scanning provides high accuracy but is constrained by high cost, sample size constraints, and limited accessibility.[12–14] Electronic thickness gauges are among the most accurate and convenient tools available, allowing for direct manual measurement,[15] but are prone to error due to the difficulty of consistent gauge positioning due to the aligner's irregular shape and operators' cognitive difference (Figure S1).

To address these limitations, this study employed computer-aided design and computer-aided manufacturing (CAD/CAM) technology to develop a 3D-printed auxiliary device featuring "rails" that guide the electronic thickness gauge probes, enabling precise CA thickness measurements at key anatomical points in predetermined directions. This innovation was designed to standardize the CA thickness measurement process, and it was hypothesized that the auxiliary device-based protocol would offer a reliable method for CA thickness measurement. This hypothesis was tested by evaluating the repeatability and reproducibility of the protocol, with the aim of establishing a new foundation for quality control in aligner design, production, and clinical application.

MATERIALS AND METHODS

This study was approved by the institutional ethical committee of West China Hospital of Stomatology, Sichuan University (WCHSIRB-D-2021-282). The workflow is shown in Figure 1.

Subject and Aligner Fabrication

A total of 24 sets of digital dental models, comprising maxillary and mandibular arches, were included, and termed original digital models (D0s). The inclusion criteria were: permanent dentition, normal crown height and morphology, no defects in the tooth positions to be measured, and no surface nodules or bubbles. These D0s were 3D-printed (NOVA3D Bene3, Nova Intelligent Technology, Shenzhen, China) into physical models (P0s) that were washed in ethanol, dried, and light-polymerized for 5 minutes using the UW-01 Washing/Curing machine. CAs were fabricated from P0s using 0.75 mm-thick polyethylene terephthalate glycol (PETG) sheets (Dreve Dentamid, Germany) via a vacuum-forming machine (230 V/115 V, 50/60 Hz, Hanzhihaokangkemao, Beijing, China) with a heating temperature of 220°C, generating 24 maxillary CAs and 24 mandibular CAs.

Design and Fabrication of the Measurement Auxiliary Device (MAD)

MADs were designed on D0s using Geomagic Studio 2013 (Geomagic, New York, USA), involving the following key steps.

Selection of Measurement Points

Measurement points were identified (Table 1): occlusal points including midpoints of the incisal edges of central incisors, cusp tips of canines, buccal cusps of first premolars, and mesiobuccal cusps of first molars; surface points at midpoints of the labial/buccal and palatal/lingual surfaces; and gingival points including midpoints at the labiogingival/buccogingival and linguogingival/palatogingival margins of those teeth (Figure 2A).

Determination of Measurement Directions

Reference cylinders were created using the "Cylinder" function through each measurement point which was marked by the "Feature" function within the software. The central axis of each cylinder was aligned to bisect the mesiodistal and buccolingual dimensions for the anterior occlusal points and perpendicular to the occlusal plane for the posterior occlusal points. For surface points, each cylinder axis was positioned perpendicular to the plane tangent to the tooth surface at the measurement point (Figure 2B).

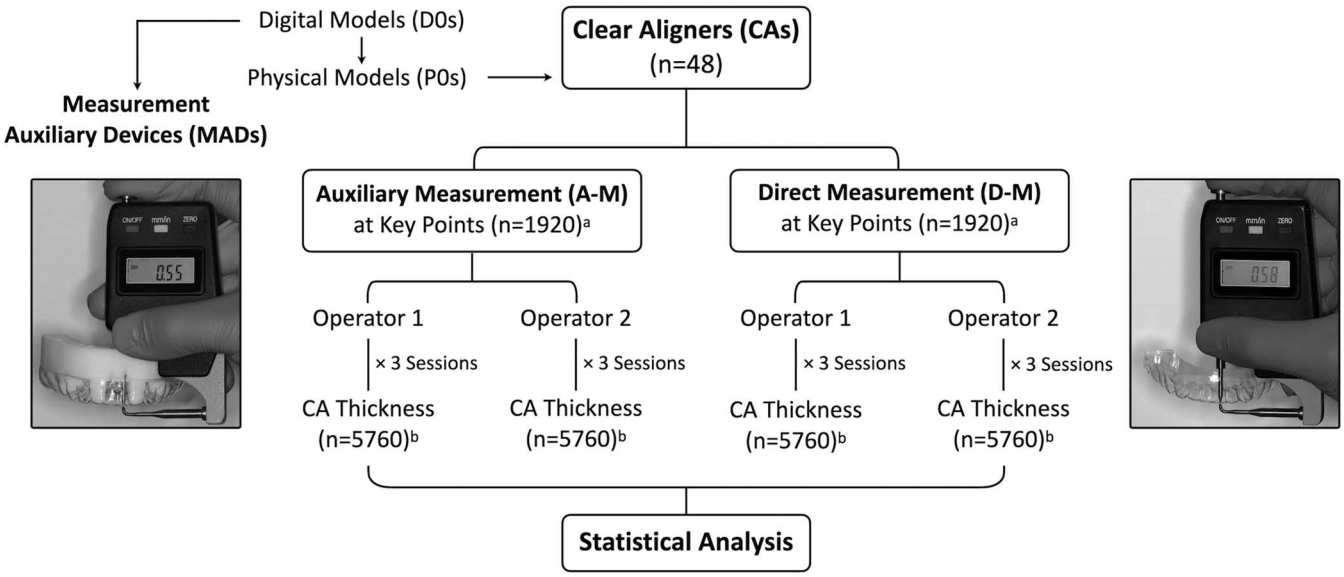

Figure 1. Flowchart of the present study. [a] n = 40 (measurement points) × 48 (clear aligners, CAs) = 1920, [b] n = 40 (measurement points) × 48 (CAs) × 3 (sessions) = 5760.

Mapping of Electronic Gauge

The electronic thickness gauge (Guanglu, Guangxi, China) was 3D scanned (UP3D, Shenzhen, China) to obtain a digital model of it, with the I-shaped probe designated as "measuring probe" and the L-shaped probe as "auxiliary probe." The digital gauge was positioned to align the contact point of the two probes with the designated measurement point. Specifically, the central axis of the measuring probe matched the reference cylinder axis for occlusal points, whereas the central axis of the auxiliary probe was aligned with the reference cylinder axis for surface points. Corresponding "auxiliary" and "measuring" cylinders were created, with diameters 0.02-mm larger than the probes (Figure 2C).

Table 1. Definition of Measurement Points on Each Clear Aligner (CA)

Measurement Point	Definition
Occlusal Point	
1-o	Midpoint of the incisal edge of the central incisor
3-o	Cusp tip of the canine
4-o	Buccal cusp tip of the first premolar
6-o	Mesiobuccal cusp tip of the first molar
Surface Point	
1-bu	Midpoint of the labial surface of the central incisor
3-bu	Midpoint of the labial surface of the canine
4-bu	Midpoint of the buccal surface of the first premolar
6-bu	Midpoint of the buccal surface of the first molar
1-pa	Midpoint of the palatal/lingual surface of the central incisor
3-pa	Midpoint of the palatal/lingual surface of the canine
4-pa	Midpoint of the palatal/lingual of the first premolar
6-pa	Midpoint of the palatal/lingual of the first molar
Gingival Point	
1-bg	Midpoint of the labial gingival margin of the central incisor
3-bg	Midpoint of the labial gingival margin of the canine
4-bg	Midpoint of the buccal gingival margin of the first premolar
6-bg	Midpoint of the buccal gingival margin of the first molar
1-pg	Midpoint of the palatal/lingual gingival margin of the central incisor
3-pg	Midpoint of the palatal/lingual gingival margin of the canine
4-pg	Midpoint of the palatal/lingual gingival margin of the first premolar
6-pg	Midpoint of the palatal/lingual gingival margin of the first molar

Generation of MAD

The digital dental arch was extended by 12 mm away from the gingival margin to form a base, with additional modules added if the measuring cylinders protruded beyond the original base. Boolean operations were performed to create insertion paths for the gauge by subtracting the measuring and auxiliary cylinders, and the teeth corresponding to the measurement points were removed to create edentulous regions, resulting in the digital MAD (Figure 2D). Each MAD was 3D printed with an ultraviolet liquid-crystal display (UV LCD) 3D printer (NOVA3D Bene3, Nova Intelligent, Shenzhen, China), with a Z-axis accuracy of 0.01 mm at a layer thickness of 0.05 mm, using High Resolution Resin (NOVA3D Bene3, Nova Intelligent, Shenzhen, China) with mechanical properties including tensile strength of 36–62 MPa, flexural strength of 59–70 MPa, Young's modulus of 1.88–2.39 GPa, and Shore D hardness of 80–85 D.

Thickness Measurement

Two operators (LQY and LJY) were trained to use the gauge with a consistent force to measure the CA thickness

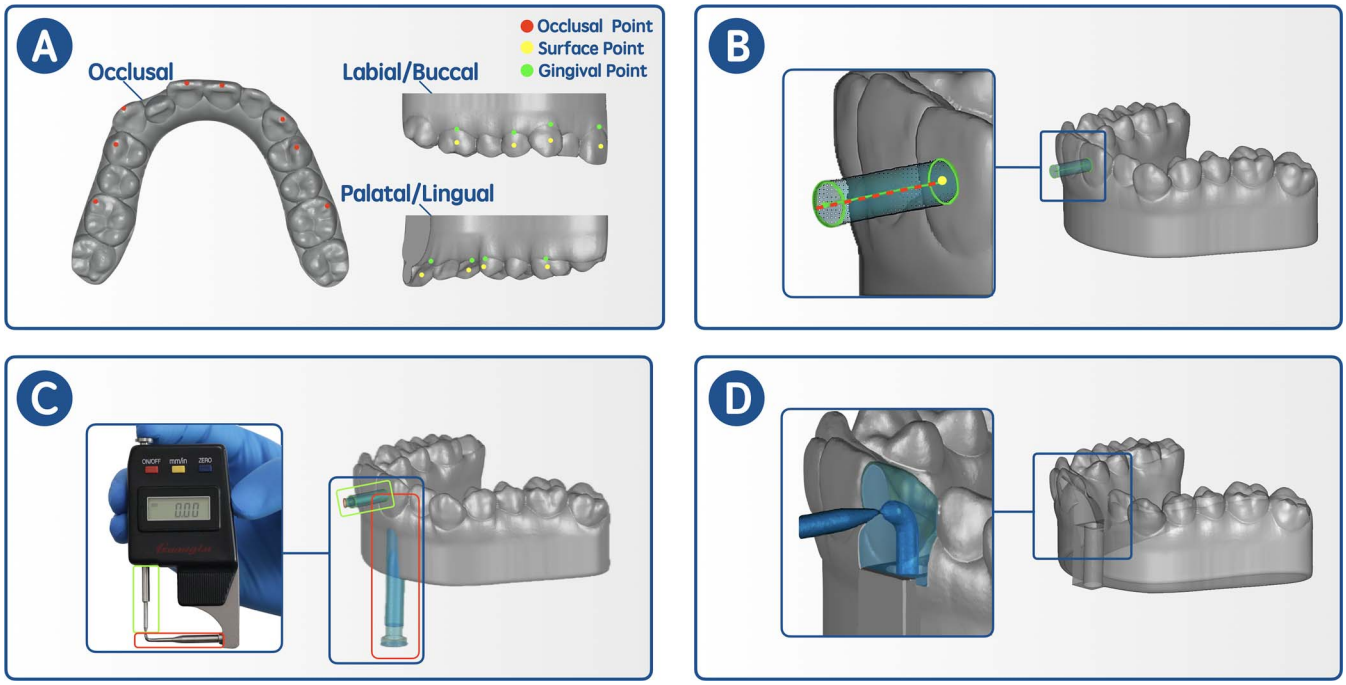

Figure 2. Design and fabrication of the measurement auxiliary device (MAD). (A) Selection of measurement points, including occlusal (red), surface (yellow), and gingival (green) points. (B) Determination of measurement directions, by creating reference cylinder (transparent blue), with its central axis (red dashed line) passing through measurement points and perpendicular to the tooth surface. (C) Mapping of electronic gauge, with the contact point of the measuring probe (circled by green) and auxiliary probe (circled by red) aligned at the measurement point, and with the measuring and auxiliary cylinders created correspondingly. (D) Generation of MAD, through Boolean operations on the measuring or auxiliary cylinders to create insertion paths for the gauge, and teeth removed to create edentulous regions.

following the manual guidelines. They conducted three sessions of independent measurements at 40 points per CA, using the electronic thickness gauge directly (direct measurement, D-M) and with the aid of the MAD (auxiliary measurement, A-M) (Figure S2). Consistent force application was practiced using training films and tare adjustment was conducted before each formal session.

Statistical Analysis

Statistical analyses were performed using SPSS 25.0 (SPSS, Inc., Chicago, USA). Shapiro-Wilk test was employed to assess data normality. Normally distributed data were described as means ± standard deviations (SDs) and non-normally distributed data as medians ± interquartile ranges (IQRs). Measurements from incisors and canines were categorized as anterior, and those from premolars and molars as posterior.

Intersession repeatability of the three measurements was calculated using repeated-measures analysis of variance (ANOVA) for normally distributed data and Friedman test for non-normally distributed data, with a significance level of $\alpha = 0.05$. Intraclass correlation coefficients (ICCs) were calculated to evaluate the inter-session repeatability and interoperator reproducibility, with ICCs indicating poor (<0.4), moderate (0.4–0.75), and good (>0.75) repeatability. Bland-Altman analysis was performed to evaluate intersession agreement by conducting pairwise comparisons for each pair of the three measurements. With 24 subjects and 40 observations each, the study provided 86% power to detect an ICC of 0.9, based on an F-test with a significance level of 0.05.

RESULTS

Intersession Repeatability

As shown in Tables 2 and 3, A-M demonstrated superior intersession repeatability with consistently higher ICCs compared to D-M across measurement points. For Operator 1, the ICCs for maxillary measurements were 0.829 for D-M and 0.994 for A-M; for mandibular measurements, the ICCs were 0.888 for D-M and 0.992 for A-M (Table 2). Similar trends were observed for Operator 2 with maxillary ICCs of 0.755 for D-M and 0.990 for A-M, and mandibular ICCs of 0.851 for D-M and 0.988 for A-M (Table 3).

When the points were individually inspected, A-M consistently achieved ICCs above 0.9 across all points, whereas ICCs for D-M reached 0.90 only at maxillary 1-pg/3-pg, 4-pa/6-pa, 4-pg/6-pg, and mandibular 4-pg/6-pg for Operator 1 (Tables 2 and 3). Bland-Altman plots confirmed the superior consistency of A-M, showing narrow 95% limits of agreement (LoA) with minimal outliers vs

Table 2. Intersession Repeatability of Thickness Measurement With Different Measurement Protocols for Operator 1[a]

	Maxillary CA				Mandibular CA			
	ICC		*P* Value		ICC		*P* Value	
	D-M	A-M	D-M	A-M	D-M	A-M	D-M	A-M
Occlusal Points								
1-o/3-o	0.603	0.991	.248	.571	0.788	0.986	0*	.001*
4-o/6-o	0.535	0.983	0*	.272	0.762	0.988	0*	.095
Surface Points								
1-bu/3-bu	0.729	0.988	0*	.460	0.839	0.959	0*	.875
4-bu/6-bu	0.607	0.985	.004*	.289	0.877	0.987	0*	.157
1-pa/3-pa	0.884	0.993	.002*	.579	0.832	0.978	0*	.607
4-pa/6-pa	0.940	0.996	.051	.657	0.876	0.989	0*	.441
Gingival Points								
1-bg/3-bg	0.816	0.992	0*	.06	0.820	0.981	0*	.153
4-bg/6-bg	0.699	0.989	.002*	.198	0.804	0.989	.102	.005*
1-pg/3-pg	0.921	0.997	.001*	.837	0.824	0.982	0*	0*
4-pg/6-pg	0.939	0.995	.020*	.921	0.905	0.991	0*	.013*
Overall	0.829	0.994	0*	.084	0.888	0.992	0*	0*

* *P* values were calculated using repeated-measures analysis of variance (ANOVA) or Friedman test for the three sessions of measurement. Differences with $P < .05$ are considered statistically significant among three measurement times (marked with *).

[a] CAs indicates clear aligners; D-M, direct measurement; A-M, auxiliary measurement; ICC, intraclass correlation coefficient.

much wider 95% LoA for D-M with frequent outliers (Figure 3). Additionally, no significant inter-session differences were detected at most points with A-M for either operator (repeated-measures ANOVA/Friedman, $P > .05$), indicating high repeatability.

Interoperator Reproducibility

Analysis of 24 maxillary CAs revealed higher interoperator reproducibility with A-M, where all ICCs exceeded 0.75. By contrast, D-M, exhibited considerable variability, with only 10% of points having ICCs above 0.75, 80% ranging between 0.4 and 0.7, and 10% below 0.4 (Table 4).

DISCUSSION

Precise measurement of CA thickness is essential in orthodontics as the thickness directly affects esthetics, comfort, fit, and mechanical efficacy. This study introduced a novel CAD/CAM auxiliary device integrated with electronic gauges for CA thickness measurement, enhancing convenience, feasibility, and reliability. By standardizing the measurement protocol, this method offers a solution for aligner quality control and provides a solid foundation for future research into aligner material properties and design optimization.

Table 3. Intersession Repeatability of Thickness Measurement With Different Measurement Protocols for Operator 2[a]

	Maxillary CAs				Mandibular CAs			
	ICC		*P* Value		ICC		*P* Value	
	D-M	A-M	D-M	A-M	D-M	A-M	D-M	A-M
Occlusal Points								
1-o/3-o	0.512	0.982	.409	.758	0.775	0.987	.545	0*
4-o/6-o	0.366	0.968	.444	.065	0.752	0.990	.098	0*
Surface Points								
1-bu/3-bu	0.728	0.985	.594	.030	0.551	0.954	.113	.844
4-bu/6-bu	0.510	0.984	.043*	.002	0.720	0.968	.326	.479
1-pa/3-pa	0.745	0.992	.586	0*	0.770	0.969	0*	.201
4-pa/6-pa	0.797	0.995	.263	.007*	0.844	0.987	0*	.434
Gingival Points								
1-bg/3-bg	0.768	0.989	.018*	.001*	0.667	0.973	.006*	.587
4-bg/6-bg	0.719	0.987	.084	0*	0.751	0.966	.141	.063
1-pg/3-pg	0.782	0.994	0*	.109	0.810	0.982	0*	.007*
4-pg/6-pg	0.796	0.994	.192	.002*	0.841	0.975	0*	.019*
Overall	0.755	0.990	0*	0*	0.851	0.988	0*	0*

* *P* values were calculated using repeated-measures analysis of variance (ANOVA) or Friedman test for the three sessions of measurement. Differences with $P < .05$ are considered statistically significant among three measurement times (marked with *).

[a] CAs indicate clear aligners; D-M, direct measurement; A-M, auxiliary measurement; ICC, intraclass correlation coefficient.

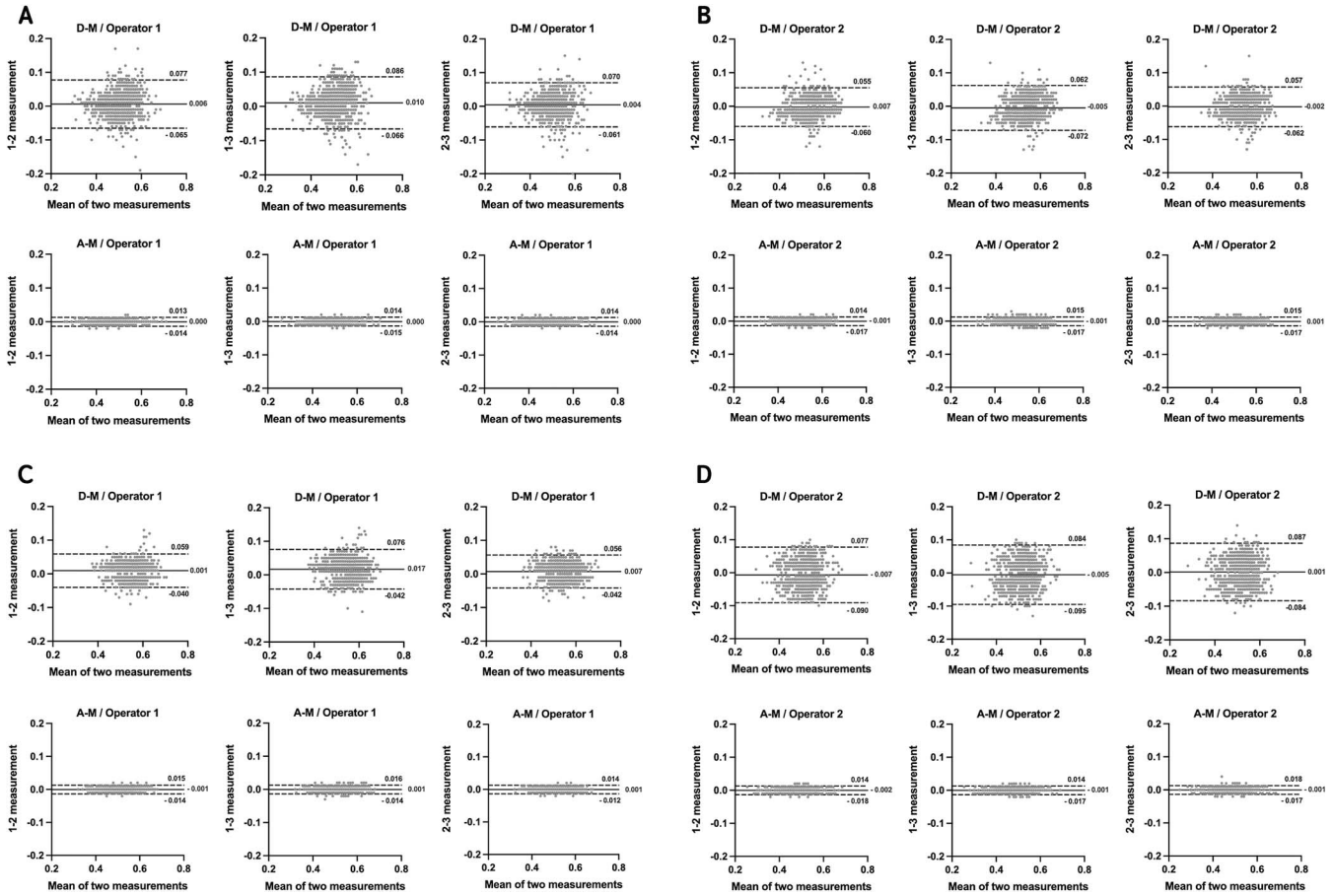

Figure 3. Bland-Altman plots for thickness measurements of (A, B) maxillary and (C, D) mandibular clear aligners (CAs) from (A, C) Operator 1 and (B, D) Operator 2, using direct measurement (D-M, upper) auxiliary measurement (A-M, lower); red line, mean difference between the two measurements; dashed blue lines, 95% limits of agreement (LoA), mean difference ± 1.96 standard deviation (SD) of the differences.

Table 4. Interoperator Reproducibility of Thickness Measurement With Different Measurement Protocols[a]

	ICCs		ICCs	
	Maxillary CAs		Mandibular CAs	
	D-M	A-M	D-M	A-M
Occlusal Points				
1-o/3-o	0.479	0.907	0.650	0.861
4-o/6-o	0.373	0.909	0.688	0.891
Surface Points				
1-bu/3-bu	0.635	0.933	0.456	0.938
4-bu/6-bu	0.465	0.839	0.581	0.946
1-pa/3-pa	0.641	0.932	0.517	0.964
4-pa/6-pa	0.798	0.950	0.503	0.976
Gingival Points				
1-bg/3-bg	0.629	0.940	0.539	0.863
4-bg/6-bg	0.519	0.880	0.571	0.965
1-pg/3-pg	0.565	0.830	0.597	0.976
4-pg/6-pg	0.692	0.953	0.593	0.978
Overall	0.684	0.916	0.725	0.968

[a] A-M indicates auxiliary measurement; CAs, clear aligners; D-M, direct measurement; ICCs, intraclass correlation coefficients.

Necessity of Targeted Thickness Measurement

The vacuum thermoforming process of CAs can lead to nonuniform shrinkage and expansion, resulting in significant thickness variations across different regions of the aligner due to varying tooth geometries, processing parameters, and material behavior.[4,5] For instance, areas such as the buccal and buccogingival surfaces are often thinner, as observed in the present study (Tables S1 and S2) and in previous studies.[16] The location-based thickness differences affect how forces are applied: thinner sections of the aligner are more flexible and exert lower forces, whereas thicker areas are stiffer and deliver higher forces.[6,12] These thickness variations necessitate targeted thickness measurements across different regions of the aligner, rather than measuring the original film or assuming a single thickness value for the entire aligner.

In this study, representative measurement points (Table 1) were selected based on their clinical relevance

to aligner performance during oral functions such as chewing, swallowing, and speaking. Excess occlusal contact at the occlusal points can cause accelerated wear, while the gingival margin areas are susceptible to deformation from frequent force during removal and reinsertion of the aligners.[17] Additionally, variations in the buccal and lingual surfaces influence comfort and overall aligner performance. Thus, a targeted approach provides a precise assessment of aligner durability and long-term fit.

Standardizing Measurement Protocol to Enhance Repeatability and Reproducibility

Current methods for measuring CA thickness face inherent limitations. Digital scanning, for instance, requires antireflective spray due to the transparency of CAs. However, consistency of this spray application is highly operator-dependent, and variations in spray thickness can introduce measurement errors, especially considering the thinness of aligners.[8–10] SEM provides high-resolution surface images but necessitates sample sectioning, which can lead to deformation and disrupt the material's integrity.[11] μCT avoids the need for sprays and sectioning but introduces challenges such as limited scan field size, high operation costs,[13,14] long processing time, and limited accessibility,[18] making it impractical for routine use despite being a gold standard for accuracy. Manual measurement with electronic gauges offers a direct approach[15] but is prone to errors, particularly due to difficulty in positioning the gauge correctly, as observed in the present study, in which large measurement variability was noted for D-M (Tables 2–4), especially in the initial attempts.

The integration of CAD/CAM technology in the present protocol addresses these challenges by enabling the design of customized MADs tailored to the anatomical structure of each tooth. This customization ensures that measurements are taken at precise, predefined points and directions, significantly reducing operator error and enhancing measurement consistency across different sessions and operators. The enhanced reliability of this protocol is evident in the A-M results, which demonstrated superior inter-session ICCs (> 0.90) and inter-operator ICCs (> 0.75) across all measured points. Additionally, A-M measures exhibited smaller SDs and IQRs compared to D-M, highlighting its consistency and precision.

Clinical Implications

Orthodontic CAs are typically made from thermoforming sheets with thicknesses ranging from 0.40 to 1.50 mm[19,20] and, after thermoforming a 0.75-mm sheet, the resulting aligner thickness is commonly reduced to 0.4 to 0.6 mm locally.[4,5,8,13,14,21] In orthodontic practice, most CA treatment utilizes movement steps of 0.25–0.33 mm,[22] whereas a threshold of approximately 0.15 mm is needed to activate tooth movement.[23,24] Based on these clinical parameters, a 0.25-mm tolerance for thickness discrepancies using superimposed digital files has been proposed,[25] with fit tolerance gaps up to 0.50 mm deemed acceptable.[8]

In the present study, the median thickness of all points measured by D-M was 0.53 mm, slightly, but significantly, greater than the 0.50-mm median by A-M ($P < .01$). Although a 0.03-mm difference is unlikely to be clinically significant on its own, the statistical significance highlights a methodological difference between the two approaches. As indicated by the Bland-Altman plots (Figure 3), the mean differences between any two sessions of measurements remained below 0.002 mm for A-M across all points but reached up to ~0.017 mm for D-M at certain points. The 95% LoA were also significantly narrower for A-M (0.027 to 0.035 mm) compared to D-M (0.099 to 0.179 mm). In practical terms, D-M readings could fluctuate by over a tenth of a millimeter and still be within normal error, whereas A-M reduced variability to just a few hundredths of a millimeter. It should be noted that session-to-session variations in the median thickness values for both A-M (up to 0.005 mm) and D-M (up to 0.024 mm) were well below the clinically acceptable thresholds reported in previous research. However, A-M protocol offers a greater margin of consistency, which is crucial for advanced applications. The proposed protocol does not aim to "fix" a wildly inaccurate manual method but, rather, to provide superior consistency and stricter quality control than current standards. By minimizing measurement error, A-M allows the detection of minor variations that D-M might overlook, enhancing data integrity and consistency across aligner batches, providing a key advantage for research and production of advanced aligner designs.

Limitations and Future Expectations

Certain aspects of the auxiliary model require attention. For example, the electronic gauge reads the thickness between two probe tips, which may introduce variability due to applied force. To mitigate this, the two operators were trained on correct force application and conducted tare adjustments before each session. Additionally, to counteract systematic errors that can arise from the 3D printing process,[26] a 0.02-mm offset was introduced to ensure smooth-without-wobbling insertion of the probe through the "rail" system to guide the gauge probe. It would be advisable to conduct preliminary experiments when employing different 3D printers or resins. It is also worth noting that the point-specific measurement approach does not capture full-surface thickness

distributions, necessitating complementary techniques for comprehensive analysis.

Looking ahead, it is envisioned that artificial intelligence (AI) algorithms could further streamline the process. Such algorithms might automate measurement point selection and orient measurement directions accordingly, reducing the manual-design time and increasing the consistency of MADs across different dental models. In addition, AI could link the measured thickness patterns to biomechanical simulations, providing a comprehensive understanding of how aligner geometry translates to force delivery.

Through analysis of thickness variation among different points, this study provided valuable data for further research and innovations in CA fabrication. The significant regional variation in thickness highlights the limitations of traditional thermoforming processes and suggests that future manufacturing methods should intentionally vary thickness to optimize aligner performance. For example, regions prone to excessive thinning could be reinforced, or intentional thinning could be used where more flexibility is desired. Recent modeling suggested that localized CA thickening in the posterior area can strengthen anchorage during anterior tooth retraction.[7] Designing aligners with such targeted thickness patterns could enhance force control, improve patient comfort, and increase durability of the appliance. These opportunities make thickness-controlled aligner fabrication a promising avenue for future research and clinical application.

CONCLUSIONS

- A novel standardized protocol for CA thickness measurement has been proposed, utilizing a CAD/CAM auxiliary device.
- The protocol provides consistent and precise measurements, thus aiding the quality control process in CA manufacturing.
- The reliability and accessibility of the protocol lay the groundwork for innovations in material advancement and design optimization to improve aligner functionality.

SUPPLEMENTAL DATA

Supplemental Figures 1 and 2 are available online.

Figure S1. Variations in determination of measurement (A) landmarks and (B) directions.

Figure S2. Thickness measurement using electronic thickness gauge with a measuring auxiliary device (MAD).

Supplemental Tables 1 and 2 are available online.

ACKNOWLEDGMENT

This work was supported by National Natural Science Foundation of China (82401170) and Sichuan Science and Technology Program (2025ZNSFSC0756, 2025ZNSFSC0752).

REFERENCES

1. Rossini G, Parrini S, Castroflorio T, Deregibus A, Debernardi CL. Efficacy of clear aligners in controlling orthodontic tooth movement: a systematic review. *Angle Orthod*. 2015;85(5):881–889.
2. AlMogbel A. Clear Aligner yherapy: up to date review article. *J Orthod Sci*. 2023;12:37.
3. Elshazly TM, Bourauel C, Ismail A, et al. Effect of material composition and thickness of orthodontic aligners on the transmission and distribution of forces: an in vitro study. *Clin Oral Investig.* 2024;28(5):258.
4. Ryu JH, Kwon JS, Jiang HB, Cha JY, Kim KM. Effects of thermoforming on the physical and mechanical properties of thermoplastic materials for transparent orthodontic aligners. *Korean J Orthod*. 2018;48(5):316–325.
5. Bucci R, Rongo R, Levatè C, et al. Thickness of orthodontic clear aligners after thermoforming and after 10 days of intraoral exposure: a prospective clinical study. *Prog Orthod.* 2019;20(1):36.
6. Hahn W, Dathe H, Fialka-Fricke J, et al. Influence of thermoplastic appliance thickness on the magnitude of force delivered to a maxillary central incisor during tipping. Am J Orthod Dentofacial Orthop. 2009;136(1):12.e11–17;discussion 12–13.
7. Jin X, Tian X, Lee Zhi Hui V, Zheng Y, Song J, Han X. The effect of enhanced structure in the posterior segment of clear aligners during anterior retraction: a three-dimensional finite element and experimental model analysis. *Prog Orthod*. 2024;25(1):3.
8. Cole D, Bencharit S, Carrico CK, Arias A, Tüfekçi E. Evaluation of fit for 3D-printed retainers compared with thermoform retainers. Am J Orthod Dentofacial Orthop. 2019;155(4):592–599.
9. Edelmann A, English JD, Chen SJ, Kasper FK. Analysis of the thickness of 3-dimensional-printed orthodontic aligners. Am J Orthod Dentofacial Orthop. 2020;158(5):e91–e98.
10. McCarty MC, Chen SJ, English JD, Kasper F. Effect of print orientation and duration of ultraviolet curing on the dimensional accuracy of a 3-dimensionally printed orthodontic clear aligner design. *Am J Orthod Dentofacial Orthop*. 2020;158(6):889–897.
11. Mantovani E, Castroflorio E, Rossini G, et al. Scanning electron microscopy evaluation of aligner fit on teeth. *Angle Orthod*. 2018;88(5):596–601.
12. Palone M, Longo M, Arveda N, et al. Micro-computed tomography evaluation of general trends in aligner thickness and gap width after thermoforming procedures involving six commercial clear aligners: an in vitro study. *Korean J Orthod*. 2021;51(2):135–141.
13. Lombardo L, Palone M, Longo M, et al. MicroCT X-ray comparison of aligner gap and thickness of six brands of aligners: an in-vitro study. *Prog Orthod.* 2020;21.
14. Park S, Choi SH, Yu HS, et al. Comparison of translucency, thickness, and gap width of thermoformed and 3D-printed clear aligners using micro-CT and spectrophotometer. *Sci Rep*. 2023;13.

15. Tunc ES, Ozdemir TE, Arici S. Postfabrication thickness of single- and double-layered pressure-formed mouthguards. *Dent Traumatol.* 2013;29(5):378–382.
16. Johal A, Sharma NR, McLaughlin K, Zou LF. The reliability of thermoform retainers: a laboratory-based comparative study. *Eur J Orthod*. 2015;37(5):503–507.
17. Jindal P, Juneja M, Siena FL, Bajaj D, Breedon P. Mechanical and geometric properties of thermoformed and 3D printed clear dental aligners. Am J Orthod Dentofacial Orthop. 2019;156(5): 694–701.
18. Hutchinson JC, Shelmerdine SC, Simcock IC, Sebire NJ, Arthurs OJ. Early clinical applications for imaging at microscopic detail: microfocus computed tomography (micro-CT). *Br J Radiol.* 2017;90(1075).
19. Liu DS, Chen YT. Effect of thermoplastic appliance thickness on initial stress distribution in periodontal ligament. *Adv Mech Eng.* 2015;7(4):1108–1111.
20. Taghizadeh H, Tafazzoli-Shadpour M. Effects of mechanical properties of thermoplastic materials on the initial force of thermoplastic appliances. *J Mech Behav Biomed Mater*. 2013;83(3):476–483.
21. Min S, Hwang CJ, Yu HS, Lee SB, Cha JY. The effect of thickness and deflection of orthodontic thermoplastic materials on its mechanical properties. *Korean J Orthod*. 2010(1).
22. Kravitz ND, Kusnoto B, Agran B, Viana G. Influence of attachments and interproximal reduction on the accuracy of canine rotation with Invisalign. A prospective clinical study. *Angle Orthod*. 2008;78(4):682.
23. Faltin R, Almeida M, Kessner C, Faltin K. Efficiency, three-dimensional planning and prediction of the orthodontic treatment with the Invisalign system: case report. *R Clín Orthodon Dental Press* 2003;61–71.
24. Boyd RL, Vlaskalic V. Three dimensional diagnosis and orthodontic treatment of complex malocclusions with the Invisalign appliance. *Semin Orthod*. 2001;7:232–258.
25. Kenning KB, Risinger DC, English JD, et al. Evaluation of the dimensional accuracy of thermoformed appliances taken from 3D printed models with varied shell thicknesses: an in vitro study. *Int Orthod*.19(1):137–146.
26. Wang P, Wang Y, Xu H, et al. Effect of offset on the precision of 3D-printed orthognathic surgical splints. *Clin Oral Investig*. 2023:1–11.